# Beyond Phase Dependent Coefficients in the Modelling and Analysis of Five-Phase Synchronous Reluctance Machine

**A.Gideon. D. Umoh[1], E.G. Ekpo[2], A. Akhikpemelo[3]**

*[1]Department of Electrical Electronics Engineering, Maritime Academy of Nigeria,*
*[2]Department of Electrical Electronics Engineering, AkwaIbom state Polytechnic IkotOsurua*
*[3]Department of Electrical Electronics Engineering, Maritime Academy of Nigeria, Oron*

---

***Abstract*—In the modelling and analysis of five-phase machine, the incorporation of the third-harmonics of the air-gap magneto-motive force during inductances determination help to improve the accuracy of the obtained results. Recording an increase in torque production as compared to neglecting the third-harmonics. To representation the five-phase machine inductances takes more than a simple sinusoidal expression, as the magneto-motive force waveforms are non-sinusoidal. In utilizing the third harmonics of the air-gap magneto-motive force and avoiding transformation to a fictitious frame of reference, the direct-phase variable model (DPVM) is most suitable. In the use of the DPVM, a phase dependent parameter is normally incorporated to present a near sinusoidal model. However, the use of the PDP is an approximation to satisfy a sinusoidal waveform, making it necessary to aspire for a model that avoids this approximation. This study models the five-phase synchronous reluctance machine considering utilizing the phase dependent parameter and ignoring the phase dependent parameter, with emphasis to the torque and speed characteristics of the machine at start, on load and during a loss of phase fault. The MATLAB/SIMULINK software is used for the analysis and implementation of the direct-phase variable model of the machine. Similar performance is recorded for the both models but with higher oscillation and transient percentage difference of 0.46%, 0.1 % and 2.4% at Start, loading and on fault respectively with the PDP model for the Speed Characteristics.**

***Keywords—Sncronous Reluctance, Five-phase, Phase variable model, Phase dependent parameter***

## I. INTRODUCTION

For a synchronous reluctance machine, the reluctance torque is necessary for energy conversion, as achieving this depends on a high saliency ratio between the d-axis and the q-axis inductances.

The inductance ratio between the two magnetic directions (q-axis and d-axis) of the rotor creates a magnetic potential between these axes, which in turn determines the strength of the produced torque. The axis with the maximum magnetic reluctance is determined by the number of employed phase especially in the multi-phase system. A synchronous reluctance machine (SYNRM) has an identical stator as the induction motor but with a salient pole rotor, and similar principle of operation as the salient pole synchronous motor, but with modifications in the number of damper windings. For improved accuracy, a multi-phase machine, the winding function is modelled to resemble the actual waveform of the winding in the slots, as well as it supplied power.

The Finite Element (FE) method is known to yield accurate result, but involves detailed characteristics machine studied, nevertheless, the winding function (WF) method yield accurate result that can be compared to the finite element (FE) method [1-3], while avoiding detailed machine characteristics study. Due to the requirement of a small air-gap for a good saliency, the perfect distribution of winding in sinusoidal form in the stator periphery cannot accurately describe the process [1], thus it is of great necessity to model the actual form of the winding with minimal error.

For a simple sinusoidal expression, the representation of inductances is less complicated as seen in three-phase synchronous machine [2, 4], and as compared to higher multi-phase synchronous machine due to the accommodation of the higher harmonics [5-9].

For the five-phase machine to achieve an accurate result, a true representation of the turn and winding function, accommodating the third-harmonics of the air-gap MMF is necessary.

Neglecting the harmonics, the multi-phase inductances resemble the three-phase inductances, and are just a resemblance of the inductances with significant recorded error.

The accuracy recorded in the use of the winding function and the modified winding function approaches [10], to verifying the equality of the mutual inductances, had reduce the work load in inductance determination. The Taguchi design of experiment methodology, with optimization of each rotor parameters using analysis of variance [11, 12] was employed for rotor parameter optimization.

Accommodating the third-harmonics of the air-gap MMF [7], an acceptable result was obtained, evident in increased torque production validated by experimental process.

Despite accommodating the third harmonics of the air-gap MMF [7], the stator inductance was transform to a fictitious frame of reference instead of using the developed winding function directly thus minimizing assumption [2]. To represent these five-phase stator inductance, phase dependent co-efficient (PDP) was introduced [6], but did not account for the air-gap MMF third- harmonics accommodate. Reference [15] accounted for the third-harmonics of the air-gap MMF, validated the result by the use of FE method, but still employed the use of phase dependent co-efficient, thus giving a near sinusoidal representation of the stator inductance as compared to the actual waveform.

This study models a five-phase synchronous reluctance machine accommodating the third harmonics of the air gap MMF and avoids the use of a PDP, while considering the machine characteristic performance of speed and torque at start, synchronism, on load and loss of e-phase fault, comparing with the model using PDP accommodation the third-harmonics of the air-gap MMF.

## II. FIVE-PHASE SYNCHRONOUS RELUCTANCE MOTOR EQUATIONS

The voltage equation for a five-phase synchronous reluctance machine (SYNRM) is given in (1)

$$\frac{dI}{dt} = L(\theta_r)^{-1}\left(V - \left\{R + \omega_r \frac{dL(\theta_r)}{d\theta_r}\right\} I\right) \quad (1)$$

$$\omega_r = \frac{d\theta_r}{dt} \quad (2)$$

$$I = \left[i_{as}; i_{bs}; i_{cs}; i_{ds}; i_{es}; i_{kq}; i_{kd}\right] \quad (3)$$

$$V = \left[v_{as}; v_{bs}; v_{cs}; v_{ds}; v_{es}; v_{kq}; v_{kd}\right] \quad (4)$$

where $\theta_r$ is the rotor position.

$I$ and $V$ are the machine current and voltage matrices and are given in (3) and (4) respectively. The inductance matrix is given in (5).

$$L(\theta_r) = \begin{bmatrix} L_{ss} & L_{sr}{}' \\ \frac{2}{5}(L'_{sr})^T & L'_r \end{bmatrix} \quad (5)$$

Where,

$$L_{ss} = \begin{bmatrix} L_{asas} & L_{asbs} & L_{ascs} & L_{asds} & L_{ases} \\ L_{bsas} & L_{bsbs} & L_{bscs} & L_{bsds} & L_{bses} \\ L_{csas} & L_{csbs} & L_{cscs} & L_{csds} & L_{cses} \\ L_{dsas} & L_{dsbs} & L_{dscs} & L_{dsds} & L_{dses} \\ L_{esas} & L_{esbs} & L_{escs} & L_{esds} & L_{eses} \end{bmatrix} \quad (6)$$

$$L'_r = \begin{bmatrix} L'_{lkq} + L_{mq} & 0 \\ 0 & L'_{lkd} + L_{md} \end{bmatrix} \quad (7)$$

$$L'_{sr} = \begin{bmatrix} L_{mq}cos\theta_r & L_{md}sin\theta_r \\ L_{mq}cos\left(\theta_r - \frac{2\pi}{5}\right) & L_{md}sin\left(\theta_r - \frac{2\pi}{5}\right) \\ L_{mq}cos\left(\theta_r - \frac{4\pi}{5}\right) & L_{md}sin\left(\theta_r - \frac{4\pi}{5}\right) \\ L_{mq}cos\left(\theta_r + \frac{4\pi}{5}\right) & L_{md}sin\left(\theta_r + \frac{4\pi}{5}\right) \\ L_{mq}cos\left(\theta_r + \frac{2\pi}{5}\right) & L_{md}sin\left(\theta_r + \frac{2\pi}{5}\right) \end{bmatrix} \quad (8)$$

Where $L_{ss}$ is the stator inductances matrix, $L'_r$ is the rotor inductances matrix referred to the stator and $L'_{sr}$ is the mutual inductances matrix between the stator and the rotor referred to the stator, $L'_{lkq}$ is the rotor q-axis leakage inductance referred to the stator and $L'_{lkd}$ is the rotor d-axis leakage inductance referred to the stator.

$$R = \begin{bmatrix} R_{as} & 0 & 0 & 0 & 0 & 0 & 0 \\ 0 & R_{bs} & 0 & 0 & 0 & 0 & 0 \\ 0 & 0 & R_{cs} & 0 & 0 & 0 & 0 \\ 0 & 0 & 0 & R_{ds} & 0 & 0 & 0 \\ 0 & 0 & 0 & 0 & R_{es} & 0 & 0 \\ 0 & 0 & 0 & 0 & 0 & R_{kq} & 0 \\ 0 & 0 & 0 & 0 & 0 & 0 & R_{kd} \end{bmatrix} \quad (9)$$

R is the resistance matrix. The electromagnetic torque is given in (9)

$$T_e = \frac{1}{2} I_s{}^T \frac{\partial L_{ss}(\theta_r)}{\partial \theta_r} I_s + I_s{}^T \frac{\partial L_{sr}(\theta_r)}{\partial \theta_r} I_r \quad (10)$$

$$I_s = [i_{as},\ i_{bs},\ i_{cs},\ i_{ds},\ i_{es}]^T \quad (11)$$

$$I_r = \left[i_{qr},\ I_{dr}\right]^T \quad (12)$$

$$T_e = J\left(\frac{p}{2}\right)\frac{d\omega_r}{dt} + T_l \quad (13)$$

Where,

$I_s$ is the stator current matrix and $I_r$ is the rotor current matrix.

J is the inertia expressed in kilogram-meter square ($kg.m^2$) or joule-seconds square ($J.s^2$), while p is the no of poles of the machine.

## III. INDUCTANCE CALCULATION

Using the expression for the calculation of stator inductances [14], and as presented in (14).

$$L_{xy} = \mu_0 rl \int_0^{2\pi} N_x(\varphi) N_y(\varphi) g^{-1}(\varphi, \theta_r) d\varphi \quad (14)$$

Where $N_x(\varphi)$ and $N_y(\varphi)$ are the winding functions of phase X and Y respectively and φ is the stator circumferential position. $g^{-1}(\varphi, \theta_r)$ is the inverse air gap

function which is a function of the stator circumferential position ($\varphi$ ) and the rotor position ($\theta_r$), while l is the axial length of the air gap of the machine, r is the radius to the mean of the air gap and $\mu_0$ is the permittivity of free space. The inverse air-gap function including the third harmonic component is given in (15).

$$g^{-1}(\emptyset_s, \theta_r) = a - bcos2(\emptyset_s - \theta_r) + \frac{b}{3}cos6(\emptyset_s - \theta_r) \quad (15)$$

Where,

$$a = \frac{1}{2}\left(\frac{1}{g_a} + \frac{1}{g_b}\right) \quad (16)$$

$$b = \frac{2}{\pi}\left(\frac{1}{g_a} - \frac{1}{g_b}\right) sin\pi\beta \quad (17)$$

Where $g_a$is the main air gap length, $g_b$ is the inter-polar slot space and β is the ratio of pole arc to slot pitch.

For self-inductances, equation (19) will be of the form of (18).

$$L_{xx} = \mu_0 rl \int_0^{2\pi} [N_x(\varphi)]^2 g^{-1}(\varphi, \theta_r) d\varphi \quad (18)$$

It is observed that the stator mutual inductance has a general sinusoidal approximation form of the inductances as given in (19).

$$L_{xy} = LA_{xy} + LB_{xy}\cos(2\theta \pm \theta_v) \quad (19)$$

$$LB_{xy} = C_{a\theta v} LB \quad (20)$$

$$LA_{xy} = C_{b\theta v} LA \quad (21)$$

Where $C_{a\theta v}$ , $C_{b\theta v}$ are the phase dependent parameter, and depends on the phase shift $\theta_v$.

Where v takes the form of 0, 1 or 2, giving a phase dependent value of $cos(0)$, $cos\left(\frac{2\pi}{5}\right)$ or $cos\left(\frac{4\pi}{5}\right)$ respectively

The phase dependent parameter values of choice give rise to three models of analysis; with third harmonic of the air-gap MMF, neglecting the third harmonic of the air-gap MMF and a sinusoidal approximation formula [6].

To represent the stator winding inductances in a generalized equation, the models can be adopted as variation of the actual representation.

From a generalized equation of inductances [6],

$$L_{s5} = L_{ls} I + L_{A5} M_{a5} + L_B M_{b5} \quad (22)$$

Where the expression for $M_{a5}$ and $M_{b5}$ are given in (23) and (24) respectively.

$$M_{a5} = L_{A5}\begin{bmatrix} 1 & C_{\theta1} & C_{\theta2} & C_{\theta2} & C_{\theta1} \\ C_{\theta1} & 1 & C_{\theta1} & C_{\theta2} & C_{\theta2} \\ C_{\theta2} & C_{\theta1} & 1 & C_{\theta1} & C_{\theta2} \\ C_{\theta2} & C_{\theta2} & C_{\theta1} & 1 & C_{\theta1} \\ C_{\theta1} & C_{\theta2} & C_{\theta2} & C_{\theta1} & 1 \end{bmatrix} \quad (23)$$

The q-axis and the d-axis magnetizing inductances are given in (25) and (26) respectively.

$$L_{mq} = \frac{5}{2}(L_A + L_k) \quad (25)$$

$$L_{md} = \frac{5}{2}(L_A - L_k) \quad (26)$$

Where,

$$L_k = L_B\left(\frac{1}{2}C_{b\theta0} + C_{b\theta1} + C_{b\theta2}\right) \quad (27)$$

Ignoring the use of the Phase Dependent Coefficient (PDP), a direct phase variable model of the machine accommodating the rotor inductances can be developed by adapting the works of [5] and [6], and are given in (28) to (34).

The relationship between the windings are represented in figure 1.

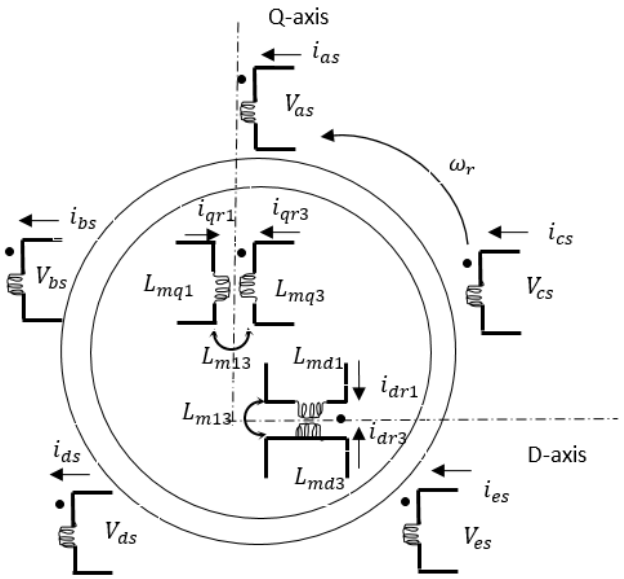


Fig.1: 5-phase machine windings showing the mutual coupling as seen in the rotor d-q circuits

In figure 1, the stator windings of the phases are considered as utilizing the fundamental and the third harmonics of MMF.

$$L'_r = \begin{bmatrix} L'_{lkq} + L_{mqs} & 0 \\ 0 & L'_{lkd} + L_{mds} \end{bmatrix} \quad (28)$$

$$L'_{sr1} = \begin{bmatrix} L_{mq}cos\theta_r & L_{md}sin\theta_r \\ L_{mq}cos\left(\theta_r - \frac{2\pi}{5}\right) & L_{md}sin\left(\theta_r - \frac{2\pi}{5}\right) \\ L_{mq}cos\left(\theta_r - \frac{4\pi}{5}\right) & L_{md}sin\left(\theta_r - \frac{4\pi}{5}\right) \\ L_{mq}cos\left(\theta_r + \frac{4\pi}{5}\right) & L_{md}sin\left(\theta_r + \frac{4\pi}{5}\right) \\ L_{mq}cos\left(\theta_r + \frac{2\pi}{5}\right) & L_{md}sin\left(\theta_r + \frac{2\pi}{5}\right) \end{bmatrix} \quad (29)$$

$$L'_{sr3} = \begin{bmatrix} L_{mq3}cos3\theta_r & L_{md3}sin\theta_r \\ L_{mq3}cos3\left(\theta_r - \frac{2\pi}{5}\right) & L_{md3}sin3\left(\theta_r - \frac{2\pi}{5}\right) \\ L_{mq3}cos3\left(\theta_r - \frac{4\pi}{5}\right) & L_{md3}sin3\left(\theta_r - \frac{4\pi}{5}\right) \\ L_{mq3}cos3\left(\theta_r + \frac{4\pi}{5}\right) & L_{md3}sin3\left(\theta_r + \frac{4\pi}{5}\right) \\ L_{mq3}cos3\left(\theta_r + \frac{2\pi}{5}\right) & L_{md3}sin3\left(\theta_r + \frac{2\pi}{5}\right) \end{bmatrix} \quad (30)$$

$$L'_{sr13} = \begin{bmatrix} L_{m13}cos3\theta_r & L_{m13}sin\theta_r \\ L_{m13}cos3\left(\theta_r - \frac{2\pi}{5}\right) & L_{m13}sin3\left(\theta_r - \frac{2\pi}{5}\right) \\ L_{m13}cos3\left(\theta_r - \frac{4\pi}{5}\right) & L_{m13}sin3\left(\theta_r - \frac{4\pi}{5}\right) \\ L_{m13}cos3\left(\theta_r + \frac{4\pi}{5}\right) & L_{m13}sin3\left(\theta_r + \frac{4\pi}{5}\right) \\ L_{m13}cos3\left(\theta_r + \frac{2\pi}{5}\right) & L_{m13}sin3\left(\theta_r + \frac{2\pi}{5}\right) \end{bmatrix} \quad (31)$$

Where $L_{mqs} = L_{mq1} + L_{mq3} + L_{mq13}$ (32)

$$L_{mds} = L_{md1} + L_{md3} + L_{md13} \quad (33)$$

$$L'_{sr} = L'_{sr1} + L'_{sr3} + L'_{sr13} \quad (34)$$

## IV. SIMULATION OF THE DYNAMIC PROCESS

The considered five-phase SYNRM design parameters are given in table 1.

TABLE I. SYNRMMACHINE DIMENSIONS AND CIRCUIT PARAMETERS

| 5-phase SRM | |
|---|---|
| Quantities | Value |
| Stator Outer / inner radius | 105.02 / 67.99mm |
| Rotor Radius | 67.69mm |
| Effective stack length | 160.22mm |
| Number of slot | 40 |
| Number of turns | 64 |
| Main air-gap length $g_a$ | 20.4mm |
| Inter polar slot space $g_b$ | 21.3mm |
| Stator slot depth | 18mm |
| Stator Slot pitch | $9^0$ |
| Ratio Pole arc / Pole pitch | 2/3 |
| Number of poles | 4 |
| Frequency | 50Hz |
| The stator resistance $R_s$ | 0.83Ω |
| Stator leakage inductance $L_{ls}$ | 10.98mH |
| rotor q-axis leakage inductance $L_{lqr}$ | 6.2mH, |
| Rotor q-axis leakage inductance $L_{ldr}$ | 5.5mH |
| Rotor q-axis resistance $R_{qr}$ | 0.25 Ω |
| rotor d-axis resistance $R_{dr}$ | 0.12 Ω |
| moment of inertia J | 0.089kg/m2 |
| phase voltage $V_{5ph}$ | 370v |

$$\boldsymbol{M_{b5}} = \begin{bmatrix} C_{b\theta 0}\cos(2\theta_r) & C_{b\theta 1}\cos(2\theta_r-\theta_1) & C_{b\theta 2}\cos(2\theta_r-\theta_2) & C_{b\theta 2}\cos(2\theta_r+\theta_2) & C_{b\theta 1}\cos(2\theta_r+\theta_1) \\ C_{b\theta 1}\cos(2\theta_r-\theta_1) & C_{b\theta 0}\cos(2\theta_r-\theta_2) & C_{b\theta 1}\cos(2\theta_r+\theta_2) & C_{b\theta 2}\cos(2\theta_r+\theta_1) & C_{b\theta 2}\cos(2\theta_r) \\ C_{b\theta 2}\cos(2\theta_r-\theta_2) & C_{b\theta 1}\cos(2\theta_r+\theta_2) & C_{b\theta 0}\cos(2\theta_r+\theta_1) & C_{b\theta 1}\cos(2\theta_r) & C_{b\theta 2}\cos(2\theta_r-\theta_1) \\ C_{b\theta 2}\cos(2\theta_r+\theta_2) & C_{b\theta 2}\cos(2\theta_r+\theta_1) & C_{b\theta 1}\cos(2\theta_r) & C_{b\theta 0}\cos(2\theta_r-\theta_1) & C_{b\theta 1}\cos(2\theta_r-\theta_2) \\ C_{b\theta 1}\cos(2\theta_r+\theta_1) & C_{b\theta 2}\cos(2\theta_r) & C_{b\theta 2}\cos(2\theta_r-\theta_1) & C_{b\theta 1}\cos(2\theta_r-\theta_2) & C_{b\theta 0}\cos(2\theta_r+\theta_2) \end{bmatrix} \quad (24)$$

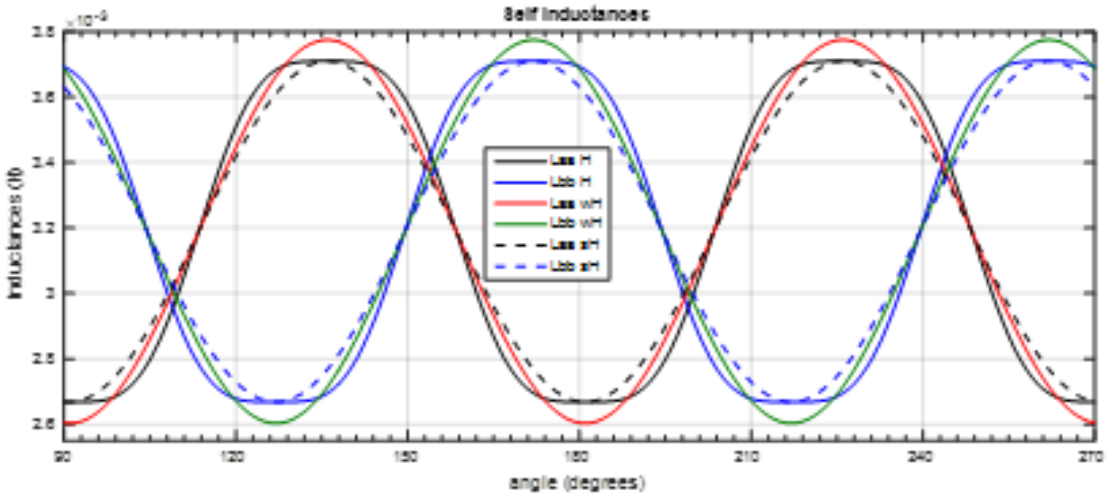


Fig. 2.5-ph stator self-inductances

The modelled 5-ph Synchronous Reluctance Machine is started directly on-line, loaded at 2.5 seconds with a load torque of 10N-m after synchronism. At 4 seconds, a loss of e-phase fault was created and subsequently restored after a second. Investigation of the machine characteristics of torque and speed was documented and compared for both the phase variable models of using a PDP (model I) and not using PDP (model II).

The speed characteristics of the models are presented in Fig. 3, with the Fig.4 and Fig.5 showing the transient at start and loading respectively. Fig.6 and Fig.7 shows the transient on start of e-phase fault and on restoration of the e-phase fault respectively for both models.

At start, the Speed performance characteristics shows a higher transient rise of 321.4 rad/s for model I as compared to 345.4 rad/s for model II, thus recording a 38.96 % oscillation for model I as compared to 18.24 % for model II.

On loading, model I speed characteristics show a higher percentage oscillation of 8.09 % about the synchronous speed as compared to 7.99 % for model II. It can be observed that the maximum transient recorded for the difference in speed characteristics between the models on loading is 0.1 %.

At loss of e-phase fault, a lower Speed oscillation rise of 12.83 % about the synchronous speed is observed for model I as compared to 15.25 % rise for model II, recording a percentage difference of 2.4 % between the models at fault.

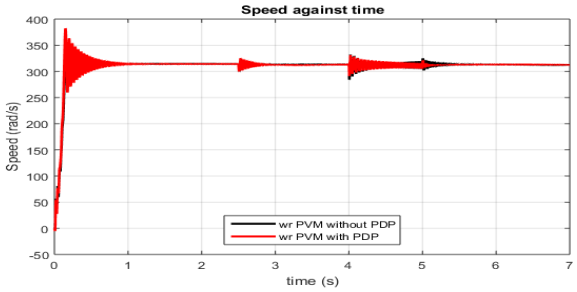


Fig. 3.Speed Characteristics

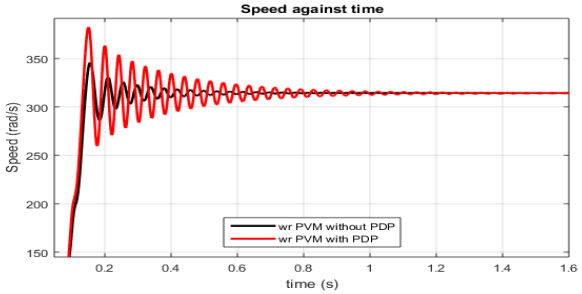


Fig. 4.Speed Characteristics (Transient at start)

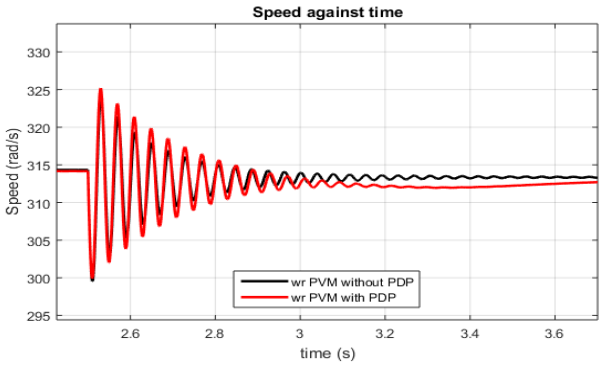


Fig. 5. Speed Characteristics (Transient at Loading)

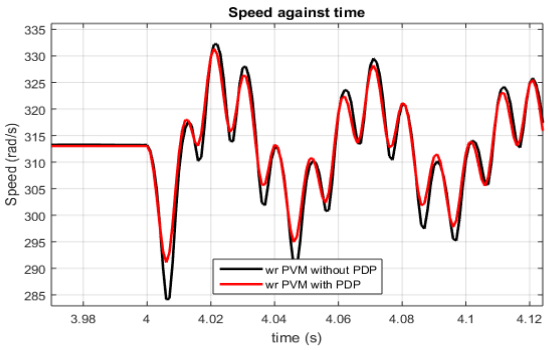


Fig. 6. Speed Characteristics (Transient at Loss of e-Phase initiated)

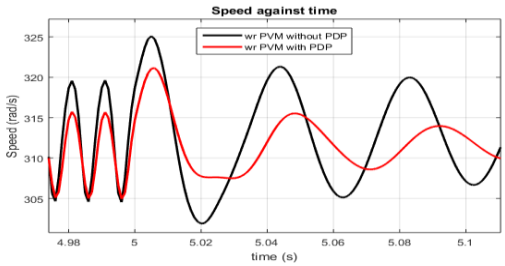


Fig. 7. Speed Characteristics (Transient on restoration of e-Phase)

The Torque characteristics of the models (Fig. 8), transient at start (Fig.9), transient on loading (Fig.10), transient on the start of e-phase fault (Fig.11) and subsequent restoration of the e-phase fault (Fig. 12) present a comparative plots of the models.

At start, the torque transient performance characteristics for model I having a value of 36.59 Nm value show greater rise as compared to 29.71 Nm for model II, thus recording an 18.8 % difference in maximum oscillation between models at start. Similarly, minimum transient rise of -33.14Nm is observed in model I as compared to a -23.81Nm value rise for model II, thus recording a 28.15 % difference for the minimum transient rise at start.

On loading, model I torque characteristics show a torque transient difference of 2.69 % in maximum oscillation value between the models. A greater value for the difference in minimum torque on loading is 31.95% between the models.

At loss of e-phase fault, a lower Speed oscillation rise between the models is 19.52 % while the minimum rise between the models is 42.91 %.

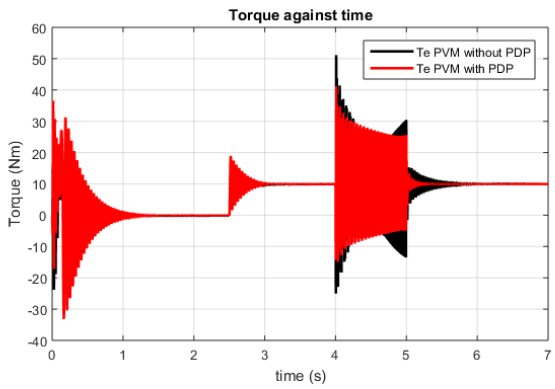


Fig. 8 Torque characteristics (With and Without PDP)

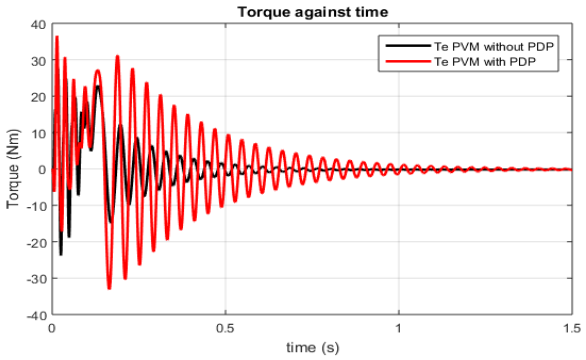


Fig. 9. Torque characteristics (Transient at start)

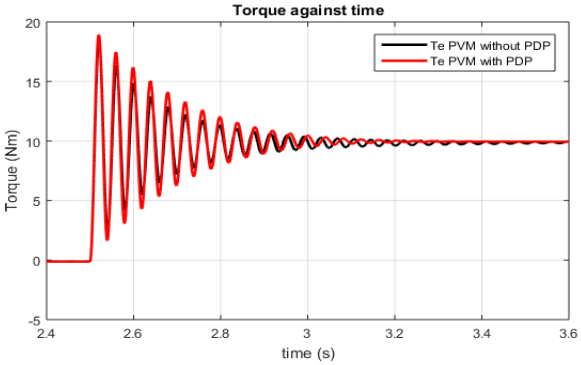


Fig. 10. Torque characteristics (Transient at loading)

An enlarge view of the plot of the torque characteristics before loading after synchronous speed is attained is presented in Fig. 10, while the plot of the torque

characteristics on start of fault and subsequent restoration of e-phase are presented Fig. 11 and Fig. 12 respectively.

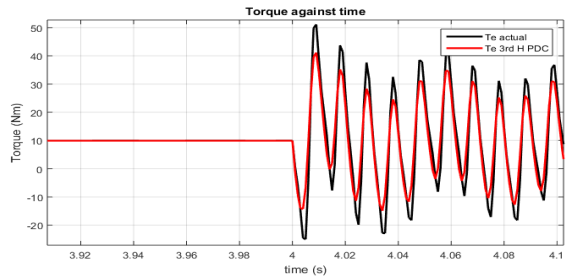


Fig. 11. Torque characteristics (at start of loss of e-phase fault)

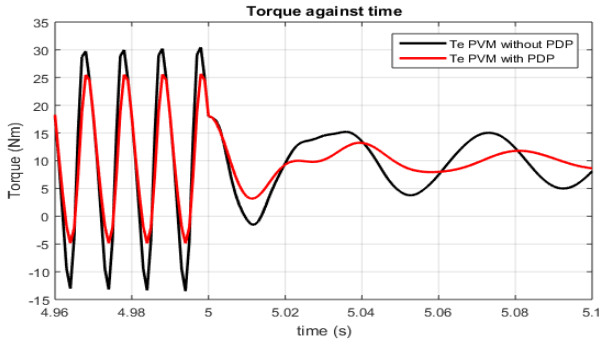


Fig. 12. Torque characteristics (Torque oscillations during loss of phase and subsequent restoration)

The performance characteristics of the different models of without PDP and PDP of speed and torque are tabulated in table II and table III respectively.

TABLE II. SPEEDPERFORMANCE CHARACTERISTICS

| Speed Characteristics (rad/s) | Start | Loading | Fault |
|---|---|---|---|
| | Transient(max – min) | Transient(max – min) | Transient(max – min) |
| PVM (PDP) | 382.4 - 260 | 325.2 – 299.8 | 331.4 – 291.1 |
| PVM Without PDP | 345.4 – 288.1 | 324.6 – 299.5 | 332.2 – 284.3 |

TABLE III. TORQUE PERFORMANCE CHARACTERISTICS

| Torque Characteristics (N-m) | Start | Loading | Fault |
|---|---|---|---|
| | Transient(max – min) | Transient(max – min) | Transient(max – min) |
| PVM (PDP) | 36.59 – -33.14 | 18.94 – 1.64 | 41.16 – -14.29 |
| PVM Without PDP | 29.71 – -23.81 | 18.43 – 2.41 | 51.14 – -25.03 |

To a greater percentage, the period between the models during transient is constant despite the change in oscillations value as shown in Fig. 13.

Both models of utilizing the phase dependent coefficient and not incorporating the phase dependent parameter still settles at the synchronous speed even though the settling times varies between the models. The model without PDP settles after transient at start at 1.3 seconds as compared to a recorded value of 1.97 seconds for the model utilizing PDP.

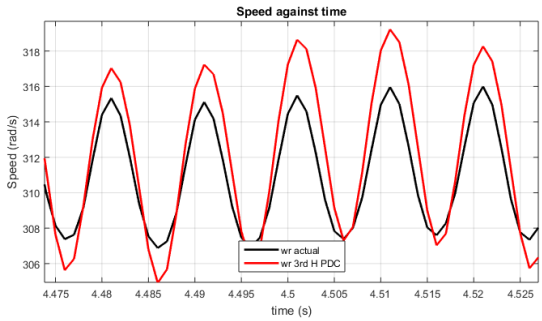


Fig. 13 Speed performance characteristics (speed fluctuations during loss of phase)

## V. CONCLUSION

The effect of the third harmonic component of the air-gap MMF has been accommodated in both models, but when utilizing the phase dependent parameter, a higher percentage of oscillation is observed as compared to the model without phase dependent parameter. percentage difference in transient of 0.46%, 0.1 % and 2.4% at Start, loading and on fault respectively with the PDP model for the Speed Characteristics. Both models have the same value at synchronism before loading and after the loss of phase fault is restored. Despite observed oscillation in model PDP, it takes longer time to settle at start but lesser settling time on loading, as compared to observation with the model without PDP. On restoration of the loss of phase fault, an increase in phase shift is observed with the PDP model having a shift of $42^0$ for the first out of phase oscillation, and damped faster as compared to the without PDP.

Considering the observed oscillations, variance in amplitude is between the models as the angle of oscillation is maintained. This is an indication that the PDP model, while presenting an approximation of the stator inductances in a sinusoidal form, introduced an increase in the value of the amplitude. The PDP model gives an acceptable result but a more accurate result is given with the model that neglect the use of the PDP.

## REFERENCES

[1] E. Obe, "Calculation of inductances and torque of an axially laminated synchronous reluctance motor," 2010, IET Electr. Power Appl., vol. 4, no. 9, pp. 783-792.

[2] E. Obe and A. Binder, "Direct-phase-variable model of a synchronous reluctance motor including all slot and winding harmonics," Energy Conversion and Management, Vol. 52 pp 284-291. 2011.

[3] E. Obe, "Direct Computation of AC machine Inductances based on winding function Theory," Energy Conversion and Management, vol. 50, pp 539-542, 2009.

[4] P. Krause, O. Wasynczuk and S. Sudhoff, Analysis of Electric Machinery, New York, IEEE press, 1995.

[5] H. Toliyat, S. Waikar andT.Lipo, "Analysis and Simulation of Five-Phase Synchronous Reluctance Machine Including Third Harmonic of Airgap MMF,"IEEE Trans. on Ind. Application, vol. 34, no. 2, pp. 332-339, 1998.

[6] T. Camarano, T. Wu, S. Rodriguez, J. Zumberge and M. Wolff "Design and Modeling of a Five-Phase Aircraft Synchronous Generator with High Power Density," IEEE Energy Conversion and Exposition (ECCE), pp. 1878 – 1885, 2012.R. Nicole, "Title of paper with only first word capitalized," J. Name Stand. Abbrev., in press.

[7] H. Toliyat, M. Rahimian, and T. Lipo, "DQ Modeling of Five Phase Synchronous Reluctance Machine Including Third Harmonic of Air-Gap MMF," IEEE Industry Applications Society Annual Meeting, vol. 1, pp 231-237, Sep/Oct 1991.M. Young, The Technical Writer's Handbook. Mill Valley, CA: University Science, 1989.

[8] G. Umoh, and E. Obe, "Five-Phase Synchronous Reluctance Motor: A better alternative to the three five Synchronous motor," ICEPENG, pp. 56- 61, Oct. 2015.

[9] G. Umoh, and E. Obe, "Analysis of Five-Phase Synchronous Reluctance Motor under loaded and faulted conditions," ICEPENG, pp. 37- 43, Oct. 2015.

[10] Toliyat, H., Nandi,S., Choi, S. *et al.*: 'Electrical Machines Modelling, Condition Monitoring, and Fault Diagnosis', CRC Press, Taylor & Francis Group, 2013.

[11] H. Azizi and A. Vahedi, "Sensitivity Analysis and Optimum design for the Stator of Synchronous Reluctance Machine using the coupled finite and Taguchi method," Turkish Journal of Electrical and Computer Sciences, vol. 23 pp 38-51, 2015.

[12] H. Azizi and A. Vahedi, 'Rotor Geometry Parameter Optimization of Synchronous Reluctance Motor using Taguchi Method', Przeglad Elektrotechniczny, vol. 89, pp 127-201, 2013.

[13] L. A. Pereira, C C. Scharlau, L. F. A. Pereira and S. Haffner "Influence of Saturation on the Airgap Induction Waveform of Five-Phase Induction Machines," IEEE Transactions on Energy Conversion, vol. 27, no. 1, pp 29-41, 2012.

[14] N. Schmitz and D. Novotny,Introductory Electromechanics, New York, The Ronald Press Com., 1965.

[15] G. D. Umoh, E. S. Obe and O.I. Okoro, "The Effect of Third-Harmonics of the Air-gap MMF on Inductance Determination in five-phase Synchronous Reluctance Motor," IEEE 3rd Conference on Electro-Technology for National Development (NIGERCON), pp. 795-801,2017.